

Geometrical consequences of kissing stents and the Covered Endovascular Reconstruction of the Aortic Bifurcation configuration in an in vitro model for endovascular reconstruction of aortic bifurcation

Erik Groot Jebbink, MSc,^{a,c} Frederike A. B. Grimme, MD,^a Peter C. J. M. Goverde, MD,^d Jacques A. van Oostayen, MD,^b Cornelis H. Slump, PhD,^c and Michel M. P. J. Reijnen, MD, PhD,^a Arnhem and Enschede, The Netherlands; and Antwerp, Belgium

Objective: Kissing stents (KS) are commonly used to treat aortoiliac occlusive disease, but patency results are often lower than those of isolated stents. The Covered Endovascular Reconstruction of the Aortic Bifurcation (CERAB) technique was recently introduced to reconstruct the aortic bifurcation in a more anatomical and physiological fashion. The aim of this study is to compare the geometrical consequences of various stent configurations in vitro.

Methods: Anatomic vessel phantoms of the aortoiliac bifurcation were created to accommodate stent configurations. Self-expandable nitinol KS, balloon-expandable covered KS, and two versions of the CERAB configuration were deployed, one with the iliac legs positioned inside the tapered part of the aortic cuff (1) and one with the legs deployed above this level (2). Computed tomography data were obtained to assess the geometry. The conformation ratio (D-ratio) was calculated by use of the ratio of the major and minor axes. The proximal mismatch area, mean mismatch area, and total mismatch volume were calculated.

Results: The highest D-ratios were observed in the nitinol KS and the CERAB configuration, implying an ideal “double-D” shape. The proximal and mean mismatch areas were four- to sixfold lower in the CERAB (1) configuration when compared with nitinol KS and CERAB (2), respectively, whereas the covered KS had the highest mismatch area. Nitinol and covered KS had the largest mismatch volume, whereas the mismatch volume was the lowest in the CERAB (1) configuration.

Conclusions: Although nitinol self-expandable stents have a high stent conformation, the lowest radial mismatch was found in the CERAB (1) configuration, supporting the hypothesis that the CERAB configuration is the most anatomical and physiological reconstruction of the aortic bifurcation. Within the CERAB configuration, the two limbs are ideally positioned inside the tapering portion of the cuff, minimizing mismatch. (J Vasc Surg 2015;61:1306-11.)

Clinical Relevance: Stents in kissing stent (KS) position have frequently been used to reconstruct the aortic bifurcation and several modifications exist. The 1-year primary patency rate of KS varies between 70%-100%, with a morbidity rate of 6% to 24%, including distal embolization in up to 8% of cases. The use of covered stents appears to improve patency rates. Various aspects of the KS configuration may affect patency rates, including the positioning of the stents and the discrepancy between the stented lumen and the aortic lumen, the so-called radial mismatch. The latter causes flow perturbations and thrombus formation, which, in turn, may decrease stent patency. Choosing a configuration with the lowest radial mismatch may thus be crucial.

Endovascular treatments of extensive lesions involving the aortic bifurcation are among the most challenging indications in endovascular surgery. According to existing

guidelines, surgery is the gold standard for bilateral and extensive occlusive disease on the basis of good long-term patency rates.¹ The 30-day mortality rate for an aorto-bifemoral bypass, however, is 4%, with an early local and systemic morbidity rate of 6% and 16%, respectively.² These complications justify the search for minimally invasive alternatives. Stents in kissing stent (KS) position have frequently been used to reconstruct the aortic bifurcation, and several modifications exist. The 1-year primary patency rate of KS varies between 70% and 100%, with a morbidity rate of 6% to 24%, including distal embolization in up to 8% of cases.³ The use of covered stents appears to improve patency rates.⁴ Various aspects of the KS configuration may affect patency rates, including the positioning of the stents and the discrepancy between the stented lumen and the aortic lumen, the so-called radial mismatch.⁵ The latter causes flow perturbations and thrombus formation that in turn may decrease stent patency.⁶ Choosing a

From the Departments of Surgery^a and Radiology,^b Rijnstate Hospital, Arnhem; MIRA Institute for Biomedical Technology and Technical Medicine, University of Twente, Enschede^c; and the Department of Vascular Surgery, Vascular Clinic ZNA, Antwerp.^d

Author conflict of interest: P.C.J.M.G. and M.M.P.J.R. have been paid a consulting fee by Atrium Maquet Getinge Group and are on their speaker's bureau. The study was partly funded by Maquet Getinge Group.

Reprint requests: Michel M. P. J. Reijnen, MD, PhD, Department of Surgery, Rijnstate Hospital, Wagnerlaan 55, 6815 AD Arnhem, The Netherlands (e-mail: mmpj.reijnen@gmail.com).

The editors and reviewers of this article have no relevant financial relationships to disclose per the JVS policy that requires reviewers to decline review of any manuscript for which they may have a conflict of interest.

0741-5214

Copyright © 2015 by the Society for Vascular Surgery. Published by Elsevier Inc.

<http://dx.doi.org/10.1016/j.jvs.2013.12.026>

configuration with the lowest radial mismatch may thus be crucial, and, for this reason, the Covered Endovascular Reconstruction of the Aortic Bifurcation (CERAB) technique was recently developed in an attempt to reconstruct the aortic bifurcation in a more anatomical and physiological fashion.⁷

With the use of this technique, a covered stent is expanded 15 to 20 mm above the aortic bifurcation and this stent is proximally adapted to the aortic wall with a larger balloon, thereby creating a cone-shaped stent. Two iliac covered stents are then placed in the distal conic segment and simultaneously inflated, making a tight connection with the aortic stent, as if they were molded together, thus simulating a new bifurcation. The aortic cuff covers the free-floating proximal ends of the iliac stents that reside in the distal aorta and might thus prevent unwanted flow perturbations around the protruding part of the stents, guiding the flow into the limbs like a funnel.

In the present study, we have assessed radial mismatch and stent conformation of four different stent configurations with the use of identical, in vitro, rigid phantoms to mimic the vessel anatomy. Results are discussed in view of the current available theoretical and clinical experience on stent patency in the aortoiliac region.

METHODS

To assess radial mismatch and differences in stent conformation between various stent configurations, four identical rigid aortoiliac bifurcation models were created, partly adopted from Chong et al.⁸ First, a literature survey was performed to obtain geometrical data of the aortoiliac anatomy.⁹⁻¹¹ Data from 47 cadavers and 55 biplanar angiograms were combined to obtain the key geometry features as presented in Table I. The combined data were used to create a model with the use of Computer-Aided Design (CAD) software (SolidWorks 2012; SolidWorks Corp, Concord, Mass). The final model included the abdominal aorta, the aortic bifurcation, the renal arteries, and both common iliac arteries. The CAD design was used to make a solid three-dimensional printed model of the vessel lumen, which, in turn, was used to make a silicone mold (620/TL95 silicone rubber; NKC, Harjon B.V., Dordrecht, The Netherlands). This was used to create wax castings of the vessel lumen. The spray-painted wax casting was placed inside a rectangular container. De-aerated clear silicone rubber (Sylgard 184; Dow Corning GmbH, Wiesbaden, Germany) was poured inside the container and set to dry at 35°C overnight. Thereafter, the temperature was increased to 120°C to melt the wax vessel lumen.

The stent configurations were constructed by two experienced vascular surgeons (P.G., M.R.) with the use of regular guide wires and catheters. Four different configurations were created. One bare metal kissing (BMK) stent configuration was made using two 10-mm self-expanding nitinol stents (S.M.A.R.T Control; Cordis Corp, Miami, Fla). After deployment, these nitinol stents were flushed with hot water (40°C) and dilated to ensure full deployment of the nitinol. In the second model, a kissing covered

Table I. Anatomical parameters used to design the bifurcation model

<i>Parameter</i>	<i>Dimensions, mean (standard deviation)</i>
Diam. abdominal aorta at inflow, mm	22 (3.5)
Diam. abdominal aorta at renal artery, mm	19 (3.3)
Diam. abdominal aorta at IMA, mm	17 (3.6)
Diam. abdominal aorta at bifurcation, mm	16 (1.6)
Diam. renal artery left/right, mm	6 (1.3)
Diam. CIA left/right, mm	8 (1.7)
Distance from aortic bifurcation to renal arteries left/right, mm	86 (1.7)
Length of CIA left, mm	55 (3.2)
Length of CIA right, mm	57 (6.1)
Length of renal artery left, mm	12 ^a
Length of renal artery right, mm	29 ^a
Branching angle renal artery left, degrees	65 (16)
Branching angle renal artery right, degrees	61 (17)
Take of angle CIA left, degrees	20 (5.9)
Take of angle CIA right, degrees	30 (6.8)
Angle of aorta, degrees	16 (3.3)

CIA, Common iliac artery; *Diam.*, diameter; *IMA*, inferior mesenteric artery. All vessels are symmetrically round, and dimensions are rounded to whole millimeters.

^aNo standard deviation available.

(KC) stent configuration, consisting of two 8-mm expanded polytetrafluoroethylene (ePTFE) covered stents (V12; Atrium Maquet Getinge, Hudson, NH), was placed. In the third and fourth model, a CERAB configuration was placed by use of one 12 × 61-mm covered stent that was dilated to 16 mm in the proximal two-thirds of the stent length and two 8 × 38-mm (CERAB-1) or 8 × 59-mm (CERAB-2) limbs. In the first CERAB (CERAB-1) configuration, these two limbs were placed exactly in the tapered part of the aortic cuff only (10 mm above the distal margin of the cuff), as the technique intended.⁷ In the second CERAB configuration (CERAB-2), the two limbs were deployed above the conic segment of the aortic cuff (25 mm above the distal margin of the cuff), which in theory would be a suboptimal position. All ePTFE-covered stents were submerged in water (40°C, 2 minutes) before placement, preventing rupture of the ePTFE.

The models were imaged by means of four modalities: still color photographs, X-ray photographs, computed tomography (CT) scanning, and bronchoscopic imaging (Fig 1). The photographs (A900; Sony, Tokyo, Japan) were made in the anterior-posterior direction, and the lumen of the model was filled with a solution of water and glycerol (ratio, 44:56 wt/wt) to match the refractive index of the silicone and fluid-filled vessel lumen. When the refractive index is matched, clear undisturbed photographs can be obtained. X-ray images were also obtained in the anterior-posterior position. To inspect the proximal stent geometry, a bronchoscope (EB-1970K 2.8; Pentax Corporation, Tokyo, Japan) was inserted into the model to obtain close-up photographs. CT imaging (Brilliance 40 slice; Philips Medical, Best, The Netherlands) was performed for each model. The following scan settings were

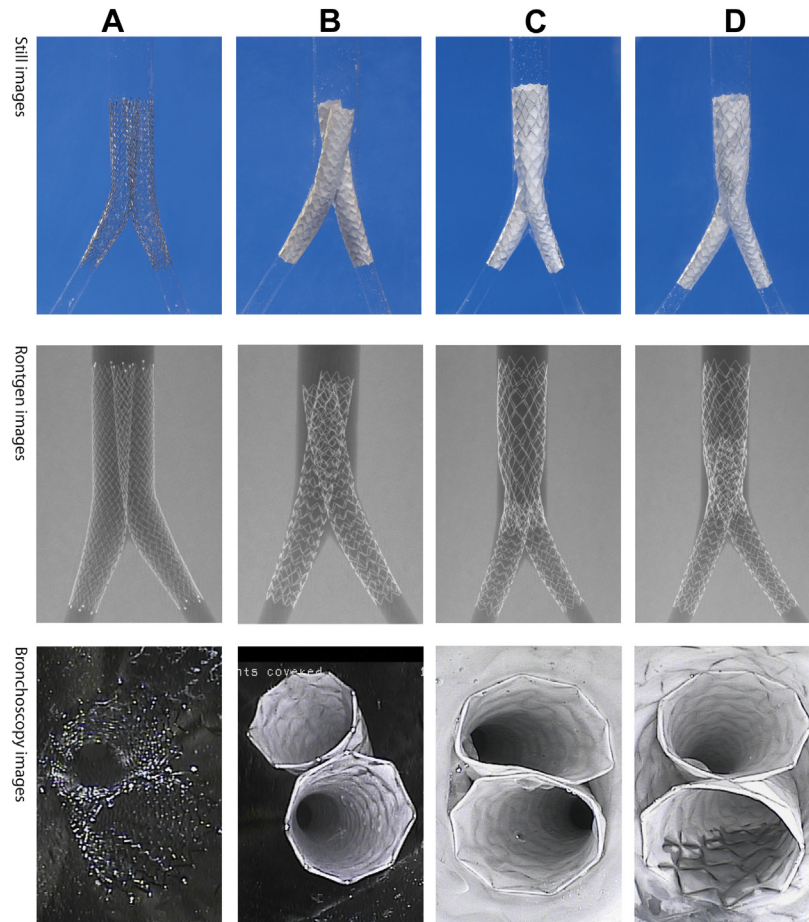


Fig 1. Still color photographs, Rontgen images, and bronchoscopic images of **A**, self-expandable nitinol kissing stents (KS); **B**, Balloon-expandable kissing covered (KC) stents; **C**, Covered Endovascular Reconstruction of the Aortic Bifurcation (CERAB)-1 with the limbs starting in the tapered part of the aortic cuff; **D**, CERAB-2 with the iliac limbs starting just above the tapered segment of the aortic cuff.

used: slice thickness 1 mm; adjacent increment; kV 120; mAs/slice 365; field of view, 180 mm. Matlab (2012A; The MathWorks Inc, Natick, Mass) was used to analyze the CT data. A software tool was designed to segment the mismatch volume in each slice by hand, with the use of a polygon approximation. All pixels within the segmented area are summed and multiplied by the pixel size to obtain the mismatch area. The proximal mismatch area was determined on the first CT slice with both limbs in view. The mean mismatch area was calculated by averaging the mismatch area determined per 1-mm slice over the entire mismatch segment. One-millimeter coupes were chosen to obtain sufficient data points for calculating the mean mismatch area. The mismatch segment is the cranio-caudal length, where a discrepancy exists between the stented lumen and the aortic lumen. The mean mismatch area was calculated as $\text{sum}(\text{mismatch area per slice})/\text{number of slices}$. The total mismatch volume was calculated summing the slice area multiplied with the slice thickness (1 mm). To assess the stent conformation

(double-D shape) ellipses (with 5 degrees of freedom: x , y , minor axes, major axes, and angle) were fitted to the stent lumen of each slice in the CT data. Thereafter, the ratio between the major and minor axes was used as a measure for stent conformation (D-ratio). Ratios higher than 1 indicate a more elliptical (or “D”) shape, with a maximum of 2. Two researchers independently performed the measurements, and the results were averaged.

RESULTS

Stent conformation. In Fig 2, the D-ratio for the four stent configurations is shown. When focusing on the inflow segment of the limbs, the BMK stents and CERAB limbs had the highest (1.6 and 1.4) D-ratios, meaning that these configurations had the highest stent conformation to the aortic wall and aortic cuff, respectively. The BMK stents retain a D-shape over the full length in the aorta, which is not seen with the other configurations. The D-ratio of the CERAB-2 rises, with a maximum of 1.6, when the limbs enter the tapered part of the aortic cuff. More proximally

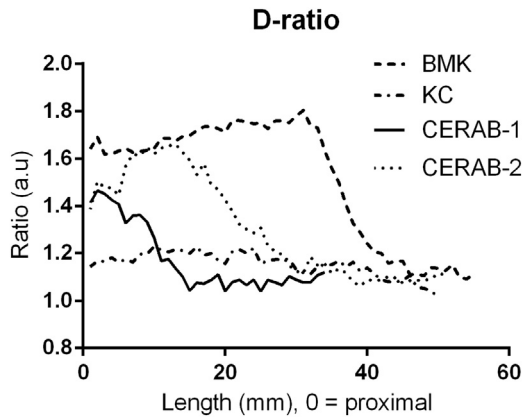


Fig 2. D-ratios of the four different configurations. A ratio of 1 indicates a circular conformation of the stent, whereas ratios higher than 1 indicate more elliptical conformation. Starting point of the graph is the proximal side of the iliac limbs. *BMK*, Bare metal kissing; *CERAB*, Covered Endovascular Reconstruction of the Aortic Bifurcation; *KC*, kissing covered.

and distally, the ratio is between 1 and 1.4, indicating a round conformation. The *KC* stents have a mean D-ratio of 1.15, pointing toward a double-barrel configuration. None of the configurations exhibited large D-ratio differences between the left and right limbs; the average difference between the left and right limbs was 0.11, 0.048, 0.036, and 0.049 for the *BMK* stents, *KC* stents, *CERAB-1*, and *CERAB-2*, respectively.

Proximal mismatch area. Fig 3 presents the axial slices of the configurations at the inflow portion of the limbs. In Fig 3, A, it is shown that the *BMK* stents are flattened in the middle, creating a double D configuration. In contrast, the *KC* stents are crossed and obtain a more round double-barrel geometry, because the kissing parts of the stents do not flatten (Fig 3, B). The limbs of the *CERAB-1* configuration (Fig 3, C) are forced into a double-D shape by the tapering part of the aortic cuff. In contrast, the *CERAB-2* configuration has a more round inflow lumen of both limbs (Fig 3, D). At the proximal inflow part, the total mismatch area was the lowest in the *CERAB-1* configuration (4.04 mm^2), compared with 24.75 mm^2 , 56.68 mm^2 , and 22.5 mm^2 for the *BMK*, *KC*, and *CERAB-2*, respectively.

Mean mismatch area. The mean total mismatch areas are presented in Table II. The *KC* stents have a mean total mismatch area (53.48 mm^2) that is more than twice that of the *BMK* stents (21.38 mm^2). The *CERAB-1* configuration has only one-sixth of the mean mismatch area (3.1 mm^2) of the *BMK* stents. The *CERAB-2* configuration has a total mean mismatch area (12.65 mm^2) that was four times that of the first *CERAB* configuration, but it was still much lower than those of the two *KS* configurations.

Total mismatch volume. The results of the three-dimensional total mismatch volume are depicted in Fig 4. The *BMK* stents have a long but straight mismatch volume

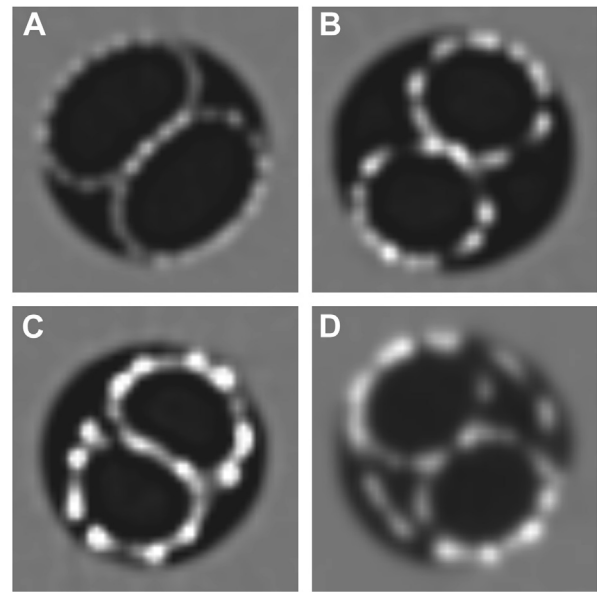


Fig 3. Axial slices of the computed tomography (CT) scans of the inflow portions of the four models. **A**, Self-expandable nitinol kissing stents (*KS*); **B**, Balloon-expandable kissing covered (*KC*) stents; **C**, Covered Endovascular Reconstruction of the Aortic Bifurcation (*CERAB*)-1 with the limbs starting in the tapered part of the aortic cuff; **D**, *CERAB-2* with the iliac limbs starting just above the tapered segment of the aortic cuff.

along the aorta. The *KC* stents had the largest mismatch volume. The mismatch volume of the *KC* stents is twisted, and the two lumina join at the bifurcation as the result of crossing of the stents. The *CERAB-1* has a thin and short total mismatch volume, whereas the *CERAB-2* has a longer, cone-shaped volume. The total volume per stent configuration can be seen in Table II. *KC* stents had the largest mismatch volume (2163.3 mm^3), whereas the mismatch volume was lowest (30.25 mm^3) in the *CERAB-1* configuration: 30 times lower than the *BMK* (903.34 mm^3). When comparing the two *CERAB* configurations, it can be seen that the mismatch volume of the *CERAB-1* configuration is almost nine times lower than that of the *CERAB-2* configuration.

DISCUSSION

Results of the present study show that different stent configurations may result in large variations in stent conformation, mismatch area (up to sixfold difference), and mismatch volume (up to 30-fold difference). The *CERAB* configuration with the limbs starting in the tapering part of the aortic cuff, as they are intended to do, was related to the best geometrical conditions, meaning the lowest radial mismatch and a high stent conformation. Both *CERAB* configurations were related to a lower mismatch area and mismatch volume when compared with the *KS* configurations, but this was above all true for the *CERAB-1* configuration. Within the *BMK* configuration, however, the D-ratio

Table II. Mean mismatch areas and volumes of the four different configurations

Configuration	Mismatch area, mm ²						Mismatch volume, mm ³		
	Prox. left	Prox. right	Prox. left + right	Mean left	Mean right	Mean left + right	Left	Right	Total
A, BMK stents	12.10	13.2	24.75	10.02	11.37	21.38	417.07	486.27	903.34
B, KC stents	27.64	30.43	56.68	26.1	27.4	53.48	1031.45	1131.85	2163.3
C, CERAB-1	2.3	1.74	4.04	1.45	1.66	3.11	14.06	16.19	30.25
D, CERAB-2	14.45	8.10	22.5	7.97	4.68	12.65	149.10	88.89	237.99

BMK, Bare metal kissing; CERAB, Covered Endovascular Reconstruction of the Aortic Bifurcation; KC, kissing covered; Prox., proximal.

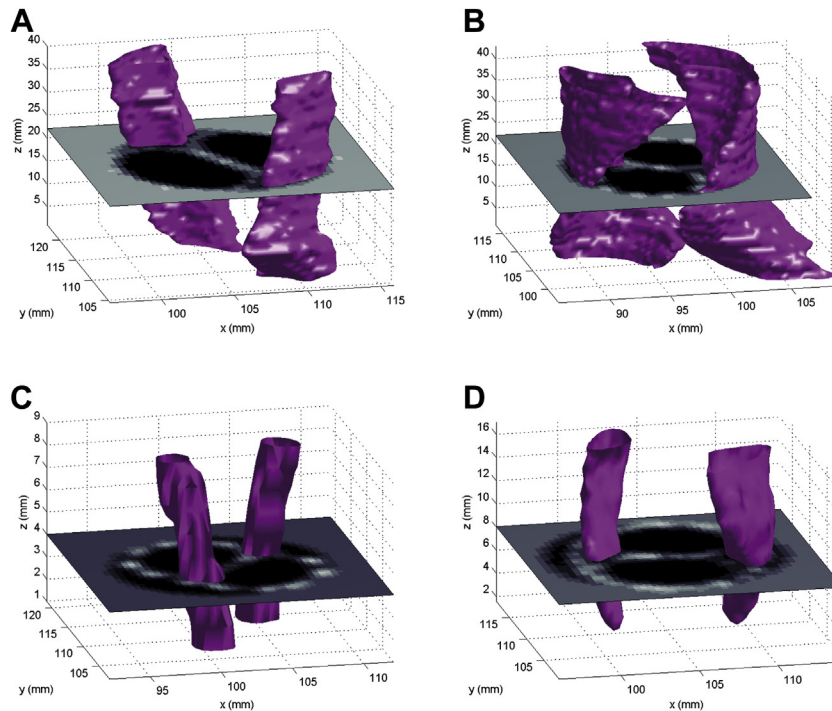


Fig 4. Geometric mismatch volumes of the four stent configurations as measured with a custom written script, used to segment the whole mismatch volume in each slice by hand, through the use of a polygon approximation. **A**, Self-expandable nitinol kissing stents (KS); **B**, Balloon-expandable kissing covered (KC) stents; **C**, Covered Endovascular Reconstruction of the Aortic Bifurcation (CERAB)-1 with the limbs starting in the tapered part of the aortic cuff; **D**, CERAB-2 with the iliac limbs starting just above the tapered segment of the aortic cuff.

was the highest, indicating that nitinol stents have the highest conformation to the vessel wall. Nevertheless, the radial mismatch was much lower in the CERAB configurations because the aortic cuff had adapted to the outline of both limbs and thus these limbs no longer need to conform to the aortic wall. Therefore, the D-ratio in these configurations is lower but eventually the radial mismatch is much lower.

Radial mismatch is considered among the most important factors affecting patency of KS.^{5,12-14} After insertion of KS, the outer stent lumen is still perfused, creating a stagnant blood column in the residual space. Previous studies have shown that the decrease in blood flow and the flow through stented vessel lumen resulted in lower shear stress associated with increased neointimal thickening.¹⁵ These findings were confirmed by the histopathological finding of mesenchymal tissue, intimal hyperplasia, and organizing

thrombus in the space between the opposing stents, within the lumen of the stents, and at the level of the stent overlapping in the distal aorta.¹³

At least two conditions of Virchow's triad are met: perturbed and stagnant flow and the inevitable endothelial damage caused by the deployed stents. Additionally, stent protrusion in the distal aorta may also influence patency, as does the crossover position of the stents.¹² These factors have not been assessed in the present study and warrant further investigation.

In our study, the KC had the highest mismatch and the lowest stent conformation ratio, which is in accord with the findings of Hughes et al.¹⁴ Clinical data, however, indicate a superiority of KC above kissing BMS.⁴ The 1- and 2-year patency rates of balloon-expandable covered stents were superior to those of balloon-expandable bare metal stents. In

the present study, however, balloon-expandable bare metal stents were not assessed. Although clinical data are still lacking, *in vitro* data suggest that the use of self-expandable nitinol KS is to be preferred above bare metal balloon-expandable stents because of significant reduction in mismatch area.¹⁴ Moreover, it is crucial to emphasize that the effect of radial mismatch on patency rates of covered stents may differ from that of bare metal stents, because the covering material will prevent flow through the radial mismatch area into the stented lumen. Obviously, this may reduce the occurrence of recirculation, turbulence, and stasis of blood. In turn, this may affect the shear stress phenomenon and thus leaves bare metal stents vulnerable to thrombosis and in-stent restenosis caused by intimal hyperplasia. Additional flow studies are indicated to elucidate this differential effect of radial mismatch on flow patterns and eventually, the patency rates of different configurations.

In this study, we have used a vascular model, based on measurements performed in cadavers. As an alternative, measurements performed on CT data could have been used, providing even more detailed anatomic information. We re-created the mean anatomic environment in which the deployed stents behaved as they would have *in vivo*. When using a straight tube model, crossing and twisting of the stents is less likely to occur, influencing the mismatch area. Nevertheless, the current model does not correct for the potential effect of calcifications and obviously, the anatomical variations in patients. Furthermore, the influence of the rigidity of the model on stent behavior is unknown and might influence the obtained results. The stents used in the current study were chosen because they represent three widely used options for aortoiliac stenting. However, many different variables can be altered when placing KS, for example, flaring of the proximal part, crossing of the stents, and increasing or decreasing the protrusion of the stents into the aorta. All of these variables could influence the mismatch area but were not taken into account in this study. We acknowledge the fact that this study only includes geometric behavior of different stent configurations. There is abundant room for further progress in determining the influences of flow and mechanical parameters in combination with several stent configurations. Furthermore, the stents were only deployed once per configuration; despite the fact that two experienced vascular surgeons deployed the stents, this may limit the reproducibility of our results. As a result, no statistical analysis could be performed on the data.

CONCLUSIONS

Although nitinol self-expandable stents had the highest stent conformation to the model wall, the lowest radial mismatch was found in the CERAB configurations, supporting the hypothesis that the CERAB configuration is a more anatomical and physiological reconstruction of the aortic bifurcation. Within the CERAB configuration, the lowest mismatch is achieved when placing the two limbs inside the tapered portion of the cuff.

AUTHOR CONTRIBUTIONS

Conception and design: EGJ, PG, CS, MR
Analysis and interpretation: EGJ, CS, MR
Data collection: EGJ, PG, MR
Writing the article: EGJ, CS, MR
Critical revision of the article: EGJ, FG, PG, JO, CS, MR
Final approval of the article: EGJ, FG, PG, JO, CS, MR
Statistical analysis: Not applicable
Obtained funding: MR
Overall responsibility: EGJ, MR

REFERENCES

1. Norgren L, Hiatt WR, Dormandy JA, Nehler MR, Harris KA, Fowkes FG, et al. Inter-Society Consensus for the Management of Peripheral Arterial Disease (TASC II). *J Vasc Surg* 2007;45(Suppl S): S5-67.
2. Chiu KW, Davies RS, Nightingale PG, Bradbury AW, Adam DJ. Review of direct anatomical open surgical management of atherosclerotic aorto-iliac occlusive disease. *Eur J Vasc Endovasc Surg* 2010;39: 460-71.
3. Grimme FA, Goverde PA, Zeebregts CJ, Reijnen MM. Reconstructing the aortic bifurcation in aorto-iliac occlusive disease. In: Greenhalgh RM, editor. *Vascular and endovascular challenges update*. London: BIBA Publishing, BIBA Medical Ltd; 2013. p. 243-51.
4. Sabri SS, Choudhri A, Orgera G, Arslan B, Turba UC, Harthun NL, et al. Outcomes of covered kissing stent placement compared with bare metal stent placement in the treatment of atherosclerotic occlusive disease at the aortic bifurcation. *J Vasc Interv Radiol* 2010;21: 995-1003.
5. Sharafuddin MJ, Hoballah JJ, Kresowik TF, Sharp WJ, Golzarian J, Sun S, et al. Long-term outcome following stent reconstruction of the aortic bifurcation and the role of geometric determinants. *Ann Vasc Surg* 2008;22:346-57.
6. Fabregues S, Baijens K, Rieu R, Bergeron P. Hemodynamics of endovascular prostheses. *J Biomech* 1998;31:45-54.
7. Goverde PC, Grimme FA, Verbruggen PJ, Reijnen MM. Covered endovascular reconstruction of aortic bifurcation (CERAB) technique: a new approach in treating extensive aortoiliac occlusive disease. *J Cardiovasc Surg (Torino)* 2013;54:383-7.
8. Chong CK, Rowe CS, Sivanesan S, Rattray A, Black RA, Shortland AP, et al. Computer aided design and fabrication of models for *in vitro* studies of vascular fluid dynamics. *Proceedings of the Institution of Mechanical Engineers Part H. J Eng Med* 1999;213:1-4.
9. Nanayakkara BG, Gunarathne C, Sanjewa A, Gajaweera K, Dahanayake A, Sandaruwan U, et al. Geometric anatomy of the aortic-common iliac bifurcation. *Galle Med J* 2007;12:8-12.
10. Shah PM, Scarton HA, Tzapogas MJ. Geometric anatomy of the aortic-common iliac bifurcation. *J Anat* 1978;126(Pt 3):451-8.
11. Moore JE Jr, Ku DN, Zarins CK, Glagov S. Pulsatile flow visualization in the abdominal aorta under differing physiologic conditions: implications for increased susceptibility to atherosclerosis. *J Biomech Eng* 1992;114:391-7.
12. Greiner A, Mühlthaler H, Neuhauser B, Waldenberger P, Dessl A, Schocke MFH, et al. Does stent overlap influence the patency rate of aortoiliac kissing stents? *J Endovasc Ther* 2005;12:696-703.
13. Saker MB, Oppat WF, Kent SA, Ryu RK, Chrisman HB, Nemcek AA, et al. Early failure of aortoiliac kissing stents: histopathologic correlation. *J Vasc Interv Radiol* 2000;11:333-6.
14. Hughes M, Forauer AR, Lindh M, Cwikiel W. Conformation of adjacent self-expanding stents: a cross-sectional *in vitro* study. *Cardiovasc Intervent Radiol* 2006;29:255-9.
15. Richter GM, Palmaz JC, Noeldge G, Tio F. Relationship between blood flow, thrombus, and neointima in stents. *J Vasc Interv Radiol* 1999;10:598-604.

Submitted Oct 31, 2013; accepted Dec 9, 2013.